IN-18
381 831

TECHNICAL NOTE
D-334

MOTION AND HEATING DURING ATMOSPHERE

REENTRY OF SPACE VEHICLES

By Thomas J. Wong, Glen Goodwin, and Robert E. Slye

Ames Research Center
Moffett Field, Calif.

NATIONAL AERONAUTICS AND SPACE ADMINISTRATION

WASHINGTON   September 1960

NATIONAL AERONAUTICS AND SPACE ADMINISTRATION

TECHNICAL NOTE D-334

MOTION AND HEATING DURING ATMOSPHERE

REENTRY OF SPACE VEHICLES

By Thomas J. Wong, Glen Goodwin, and Robert E. Slye

SUMMARY

The results of an analysis of the motion and heating during atmospheric reentry of manned space vehicles has shown the following:

1. Flight-corridor depths which allow reentry in a single pass decrease rapidly as the reentry speed increases if the maximum deceleration is limited to 10g.

2. Use of aerodynamic lift can result in a three- to fivefold increase in corridor depth over that available to a ballistic vehicle for the same deceleration limits.

3. Use of aerodynamic lift to widen these reentry corridors causes a heating penalty which becomes severe for values of the lift-drag ratio greater than unity for constant lift-drag entry.

4. In the region of most intense convective heating the inviscid flow is generally in chemical equilibrium but the boundary-layer flows are out of equilibrium. Heating rates for the nonequilibrium boundary layer are generally lower than for the corresponding equilibrium case.

5. Radiative heating from the hot gas trapped between the shock wave and the body stagnation region may be as severe as the convective heating and unfortunately occurs at approximately the same time in the flight.

INTRODUCTION

Reentry into the earth's atmosphere at circular satellite speed has been studied extensively in recent years. However, as space voyages become more ambitious and atmosphere reentry is made from flights in the vicinity of the near planets or the moon, the reentry speed will be in excess of circular satellite speed. It has been found by a number of

investigators that as the reentry speeds increase, the manned vehicle must be guided through relatively narrow corridors in order to enter in a single pass or to avoid excessive deceleration and heating (refs. 1 and 2).

It is the purpose of this paper to discuss these reentry corridors, to show how they may be widened by aerodynamic forces, and to assess the heating penalties paid for this aerodynamic widening. In addition to the main objective, the various modes of aerodynamic heating to the reentry vehicle will be discussed.

<div style="float:right">L
1
0
9
0</div>

SYMBOLS

A vehicle reference area, sq ft

C_D vehicle drag coefficient

C_{D_O} drag coefficient at zero lift

$C_{D_{MAX}}$ maximum drag coefficient

C_L vehicle lift coefficient

$C_{L_{MAX}}$ maximum lift coefficient

C_Q coefficient in total-heat equation

C_q coefficient in heating-rate equation

G_{MAX} maximum resultant deceleration, g units

g earth's gravity acceleration, 32.2 ft/sec^2

L/D vehicle lift-drag ratio

$(L/D)_{MAX}$ maximum vehicle lift-drag ratio

Q_s stagnation-point heat absorbed, Btu/sq ft

$\dot{q}_s$ stagnation-point heating rate, Btu/(sq ft)(sec)

R nose radius, ft

Re   Reynolds number

r_0 earth's radius, ft

V_E reentry velocity, ft/sec

$\overline{V}_E$ entrance velocity ratio, $\dfrac{V_E}{\sqrt{gr_0}}$

$\overline{V}_X$ exit velocity ratio or final velocity ratio in total-heat equation

W   vehicle weight, lb

Δy_p corridor depth, miles

α angle of attack, deg

REENTRY CORRIDORS

Figure 1 illustrates what is meant by a reentry corridor. A space vehicle approaching the earth is on a flight path which is a conic section until it encounters the earth's atmosphere, where the flight path will depart from the conic shape because of aerodynamic forces. The overshoot boundary is defined as the path at which the vehicle just encounters enough atmospheric drag to slow down sufficiently to enter in a single pass. Flight paths above this overshoot boundary result in a multiple pass reentry. The lower or undershoot boundary is determined by deceleration limits, usually taken as 10g for manned reentry vehicles. The corridor boundaries, however, may be further limited by heating considerations.

It is convenient to define the corridor depth as the difference in conic perigee altitude between the overshoot and the undershoot boundary. Conic perigee is the perigee the vehicle would experience in the absence of an atmosphere on the earth. For shallow reentries of the type discussed, the difference between the corridor depth defined in this way and the actual depth at the outer edge of the atmosphere is small.

Effect of Reentry Speed

The depths of these reentry corridors are functions of two parameters: L/D and the entrance speed. The effect of entrance speed on corridor depth is shown in figure 2.

In figure 2 is plotted the corridor depth for nonlifting vehicles in miles as a function of $\overline{V}_E$, the ratio of reentry speed to satellite speed. This curve was calculated by assuming a 10g maximum deceleration at the undershoot boundary. Note the very rapid narrowing of the corridor depth as the entrance speed increases. For example, at a speed 10 percent greater than local satellite speed the corridor depth is roughly 26 miles; at escape speed, the corridor has narrowed to 7 miles; and at an entrance speed of 1.6 times satellite speed, the corridor depth is somewhat less than 3 miles. These very narrow corridor depths, therefore, appear to place rather strenuous requirements on guidance system accuracy and any aerodynamic widening of these corridors which can be achieved should be extremely helpful.

For return trips from the vicinity of the moon the resulting reentry speed will be approximately escape speed or a speed ratio equal to $\sqrt{2}$ with respect to satellite speed. Therefore, the main part of this paper will be restricted to this reentry speed.

Effect of Deceleration Limits

The effect on the corridor depth of relaxing the restriction on maximum deceleration is shown in figure 3. In this figure is plotted corridor depth in miles as a function of the maximum deceleration in g units for a nonlifting vehicle. At the overshoot boundary the deceleration encountered for reentry is approximately 8g and corresponds to a zero corridor depth; as the deceleration is increased to 10g the corridor depth has opened up to about 7 miles. If a deceleration of 20g can be tolerated by the vehicle and its occupants, the corridor depth is increased to 20 miles. This curve was calculated by assuming that $W/C_D A$ of the vehicle was constant during the reentry. Substantial corridor widening can be obtained if the vehicle has a variable $W/C_D A$. For nonlifting vehicles, the flight corridor can be widened only by relaxing deceleration limits or by changing the $W/C_D A$ of the vehicle in flight.

Effect of Lift

The next point to be considered is the widening of these corridors by the use of aerodynamic lift, and this effect is shown in figure 4. Corridor depth in miles is shown as a function of the lift-drag ratio of the vehicle. The corridors shown are for reentries in which L/D is held constant at least until the flight path becomes horizontal. First, consider the lower region, which is the corridor depth for non-lifting vehicles. This corridor is the 7-mile corridor for a nonlifting vehicle experiencing a maximum deceleration of 10g. The middle shaded region represents the corridor widening brought about by lowering of the undershoot boundary through the use of positive lift. For values of the lift-drag ratio up to approximately unity, considerable widening is evident. However, at high values of the lift-drag ratio, the increase in corridor depth becomes relatively small. High values of the lift-drag ratio are ineffective simply because the resultant deceleration has been limited to 10g. If a higher maximum deceleration can be tolerated, the rising trend of this curve persists to higher values of the lift-drag ratio.

The corridor depth increase resulting from raising the overshoot boundary is shown by the upper shaded region. This results from using negative lifts to deflect the vehicle flight path downward into the denser atmosphere so that sufficient drag can be encountered to permit entry in a single pass. Note that the use of negative lift to raise the overshoot boundary is not as effective as was the use of positive lift to lower the undershoot boundary. This results from the exponential nature of the atmospheric density variation with altitude. Above certain altitudes the vehicle is unable to produce sufficiently high forces to deflect its flight path. It may now be seen that the use of lift has increased these boundaries from 7 miles for the nonlifting vehicles, for the 10g maximum deceleration, to 37 miles at an L/D of 1/2 and 50 miles at an L/D of unity.

For values of the lift-drag ratio greater than 1/2, multiple-pass entry will result if this lift-drag ratio is held constant throughout the entire reentry. However, in reference 3 it is shown that the beneficial effects of high lift-drag ratio may be realized and the vehicle kept in the atmosphere if the lift is decreased after the vehicle flight path has become horizontal.

It seems, then, that the use of aerodynamic lift can considerably widen the entrance corridors. The question now raised is what penalty is paid in terms of aerodynamic heating for this beneficial effect. Before discussing the aerodynamic heating, it is of interest to review the domains of fluid mechanics wherein maximum convective heating occurs for these vehicles and to examine their flight path with the objective

of determining whether any new mode of heat transfer appears as the
flight speeds are increased above satellite speed.

AERODYNAMIC HEATING IN CORRIDOR

Convective Heating

The flight paths of representative vehicles entering the earth's
atmosphere at escape speed are shown in figure 5. The flight paths of
three representative vehicles flying at undershoot boundary $(L/D = 1/2)$,
overshoot boundary $(L/D = -1/2)$, and in a nonlifting 10g maximum decel-
eration path are shown. Examination of a large number of vehicle paths
has indicated that the region of maximum convective heating lies within
an altitude band of from 150,000 to 250,000 feet and over a narrow speed
range. The region of maximum heating is shown by the shaded area and
the characteristics of the flow in the region will now be examined. A
curve representing flight at a constant Reynolds number of 10^6 based
upon a 10-foot length is also shown on the chart. Flight paths above
this line have Reynolds numbers of less than 10^6, and flight paths lying
below this line have Reynolds numbers greater than 10^6.

Notice that the region of severe convective heating occurs at
Reynolds numbers in the vicinity of 10^6 and, therefore, it is expected
that the flow over these bodies may be laminar. Also shown in figure 5
by the horizontal line labeled "mean-free path 5/1000 foot" is the region
where rarefaction effects would be expected to become appreciable. It
can be seen that in the region of most intense convective heating the
flow is well within the continuum regime.

It is of interest to examine the flow in the region of most intense
convective heating to determine whether the flow is in chemical equilib-
rium and also whether any new modes of heating are present which would
add to the already severe convective heating. These states of flow are
shown in figure 6 in terms of altitude as a function of velocity with
the region of maximum heating from the previous figure indicated as the
shaded rectangle. The solid line on the upper portion of the chart
divides the regions of equilibrium and nonequilibrium inviscid flow.
Flight at velocities and altitudes below this line results in flows which
are in chemical equilibrium at the boundary-layer edge for bodies having
nose radii larger than 1 foot. It appears, therefore, that the inviscid
flow will be substantially in chemical equilibrium during the regions
of most intense convective heating.

The situation is somewhat different, however, with respect to the
flow in the boundary layer. The state of the flow in the boundary layer

is shown by the lower solid curve. Flight at altitudes and velocities below this second curve result in flows which are in chemical equilibrium. Notice, however, that a large portion of the region of intense convective heating is in a region where the flow in the boundary layer is out of equilibrium. Admittedly, the boundary between equilibrium and nonequilibrium is broad. The line shown in figure 6 was chosen where the convective heating has been decreased 30 percent below its equilibrium value by nonequilibrium effects. Generally, nonequilibrium flows in the boundary layer tend to reduce the convective heat transfer below the equilibrium values for noncatalytic walls. This results from the fact that energy is contained within the gas which would normally be available for transfer to the body. Present estimates indicate reactions at the wall will be small, as ablation is very effective in reducing the number of atoms which diffuse to and strike the wall. In addition, walls which are kept reasonably cold in order to survive are covered with a layer of cold gas through which only a few atoms survive in their trip towards the surface of the body. Chung at Ames Research Center has recently developed theoretical methods which allow prediction of these heating rates over shaped blunt bodies for nonequilibrium flow conditions.

L
1
0
9
0

Radiative Heating

Also shown in figure 6 by the solid black area is the region of maximum radiative heating. This is the heating which arises from the radiation from the hot gases trapped between the bow shock wave and the body surface. In the solid black region the radiative heating is of magnitude equal to that of the convective heating. The exact magnitude depends upon the nose radius of the body and on the correctness of measured air radiation rates. The general mechanism of radiation heating will not be discussed here except to say that the radiation heating can be as important as the convective heating, and unfortunately occurs at nearly the same time in the flight.

To sum up, then, it can be seen from figure 6 that the inviscid flow over most of these reentry bodies will be in equilibrium but that the flow in the boundary layer may not be. The net result of nonequilibrium flow in a boundary layer is to reduce heat transfer to the wall for the case of an ablating wall, which appears to be the one of most practical engineering importance. Radiative heating will be severe and will occur roughly at the same time in the flight as the maximum convective heating.

8

Heating at Corridor Boundaries

There is a fundamental difference between the heating rates encountered during an overshoot boundary and an undershoot boundary. Typical heating rates for a vehicle having a lift-drag ratio of 1/2 and $W/C_D AR$ of 56 are shown in figure 7. In this figure are plotted the stagnation-point heating rates as a function of time for the overshoot-boundary flight and for flight at the undershoot boundary. Notice that the heating rate has a very high maximum at the undershoot boundary. The heating rate then drops to a low value and has a second maximum which occurs as the vehicle approaches satellite speed, after which time the heating rate is fairly low. Along the overshoot boundary the heating rates are reasonably low, but persist for fairly long periods of time. Two conditions must be dealt with by the thermal protection system: high rates existing for a short time along the undershoot boundary, and low heating rates persisting for a very long time along the overshoot boundary. In other words, the thermal protection system must be able to cope with both high heating rates for short periods and low heating rates of long duration where the total amount of heat being taken aboard the vehicle becomes quite large.

It is possible to estimate these heating rates by means of the following relatively simple relations taken from reference 1. The peak value of the heating rate is

$$\dot{q}_s = \frac{19\left(C_q \bar{V}_E\right)^2 \sqrt{\frac{W}{C_D AR}} \sqrt{G_{MAX}}}{\left[1 + (L/D)^2\right]^{1/4}} \tag{1}$$

The constant C_q has been determined from machine computations and has a value varying from unity to approximately 0.6, depending upon the flight path. The heat absorbed between $\bar{V}_E = 1.4$ and $\bar{V}_X = 1$ is,

$$Q_s = \frac{8,800\left[1 + (L/D)^2\right]^{1/4} \sqrt{\frac{W}{C_D AR}}}{C_Q \sqrt{G_{MAX}}} \tag{2}$$

The term C_Q has also been determined from machine computations and varies from unity to about 0.8, depending upon the flight path. The lift-drag ratio, which enters into these equations directly, can be seen to reduce the heating rate, as it occurs in the denominator of the upper equation, and to increase the total heat absorbed. If the vehicle lift-drag ratio were independent of the drag coefficient, estimation of the heating rates for various vehicles under various flight

conditions would be very simple. However, these two quantities are interrelated and, in order to assess the heating penalties for widening the corridors by the use of aerodynamic lift, a family of vehicles will be considered.

To illustrate this point and to demonstrate why certain modes of operation are more desirable than others from the heating standpoint, the characteristics of a set of bodies have been determined. The assumptions and the bodies used are shown in figure 8. As shown by the plan and side elevations, the bodies considered have flat-bottom delta wings with 75° of sweep. The nose diameter was taken equal to the body thickness. The drag and lift coefficients were determined from the simple Newtonian relationships shown. The minimum value of drag coefficient C_{D_0} was assumed to be the sum of the nose drag and wing leading-edge drag. The skin-friction drag was neglected in this simplified analysis. Maximum drag coefficient was taken to be 1.7 and a vehicle weight of 6,000 pounds was assumed. Figure 9 shows the calculated $W/C_D A$ as a function of the lift-drag ratio for two modes of operation: $(L/D)_{MAX}$ and $C_{L_{MAX}}$. As expected, $W/C_D A$ increased as the vehicle became thinner and was able to produce a higher value of the lift-drag ratio. Of course, flight at $C_{L_{MAX}}$ did not result in a change in $W/C_D A$.

The maximum heating rate at the undershoot boundary was calculated from equation (1) for a vehicle nose diameter equal to the body thickness. In figure 10 is shown the maximum heat-transfer rate for the stagnation region of the nose as a function of the lift-drag ratio. For vehicles operating at $(L/D)_{MAX}$, $W/C_D A$, and hence heating rate, increases with lift-drag ratio. For operation at $C_{L_{MAX}}$ the heating rates increase only slightly as the lift-drag ratio increases. This increase reflects the smaller nose diameter of the thinner bodies. The main point evident from this figure is that if high constant lift-drag ratio is to be used to widen the flight corridors, then high heating rates are to be expected.

The maximum heating rate at the stagnation point of a body is not the sole parameter used to judge the attractiveness of a particular design. One other quantity of interest is the total heat taken aboard as the vehicle is decelerated from escape speed to satellite speed, and this is shown in figure 11. Notice that as the lift-drag ratio increases, the total heat taken aboard the vehicle increases, and for the case of operation at $(L/D)_{MAX}$, this increase in total heat is significant. The final point of this study is to show the interdependence of these two parameters and to indicate the order of the heating penalty for widening reentry corridors.

Heating rate and heat absorbed at the stagnation point as functions of corridor depth are shown in figure 12. These quantities were obtained from equations (1) and (2). The corresponding corridor depths were taken from figure 4. The curves in this figure are for operation at $(L/D)_{MAX}$; heating rates are shown by the solid curve and total heat by the dashed curve. It can be seen that the heating rate and total heat absorbed begin to increase rather sharply above corridor depths of about 50 miles. This increase corresponds to operation at a value of $(L/D)_{MAX}$ of unity and for a constant value of the lift-drag ratio during the reentry. Operation at maximum lift coefficient, which was shown earlier not to yield severe heating penalties, is not shown in this figure because, as part of the simplifying assumptions, L/D at $C_{L_{MAX}}$ is a constant and the corridor depths for this mode of operation do not change. The results, however, would plot as a short vertical line and depart only a small amount from the values shown at L/D = 0.6. For operation at $(L/D)_{MAX}$, these results as summed up in figure 12 certainly indicate that if lift-drag ratios sensibly above unity are used, a relatively large heating penalty will result.

SUMMARY OF RESULTS

The results of this analysis, which was made with the assumption that the lift-drag ratio and the vehicle $W/C_D A$ were constant during the reentry, have indicated that the corridor depths through which a vehicle must be guided to avoid excessive decelerations and still make an entry in a single pass are very narrow. It is indicated that the use of aerodynamic lift can widen these corridors three- to fivefold. In addition to the widening of the corridors a vehicle capable of producing a reasonable lift-drag ratio has the advantage of being able to produce fairly sizable amounts of lateral range. The analysis of a simple family of bodies has indicated that rather severe heating penalties are paid for corridor widening for lift-drag ratios above unity. In addition to these general conditions, a survey of the modes of heat transfer in this new regime of flight speeds and altitudes has indicated that the flow over the bodies in the inviscid region between the boundary layer and the shock wave may be expected to be in chemical equilibrium; the flow will probable be laminar over at least reasonably sized bodies. Continuum flow can also be expected. It has been determined that the flow in the boundary layer may be out of equilibrium, but the net effect of this phenomenon on the heat-transfer rate for noncatalytic walls appears to be a lessening of the severity of the heating problem. An examination of the radiant energy received by the body from the hot gases contained between the shock wave and the body surface has indicated that a new mode of heating is present here which was not present for decaying satellite or ICBM reentry. Raidant heating may be as

severe as the convective heating for large bodies and unfortunately occurs at the same time in the flight.

Ames Research Center
National Aeronautics and Space Administration
Moffett Field, Calif., April 11, 1960

L
1
0
9
0

REFERENCES

1. Chapman, Dean R.: An Analysis of the Corridor and Guidance Requirements for Supercircular Entry Into Planetary Atmospheres. NASA TR R-55, 1960.

2. Wong, Thomas J., and Slye, Robert E.: The Effect of Lift on Entry Corridor Depth and Guidance Requirements for the Return Lunar Flight. NASA TN D-319, 1960.

3. Lees, Lester, Hartwig, Frederic W., and Cohen, Clarence B.: The Use of Aerodynamic Lift During Entry Into the Earth's Atmosphere. GM-TR-0165-00519, Space Tech. Labs., Inc., Nov. 20, 1958.

12

L
1
0
9
0

CONIC PERIGEE
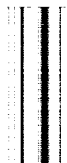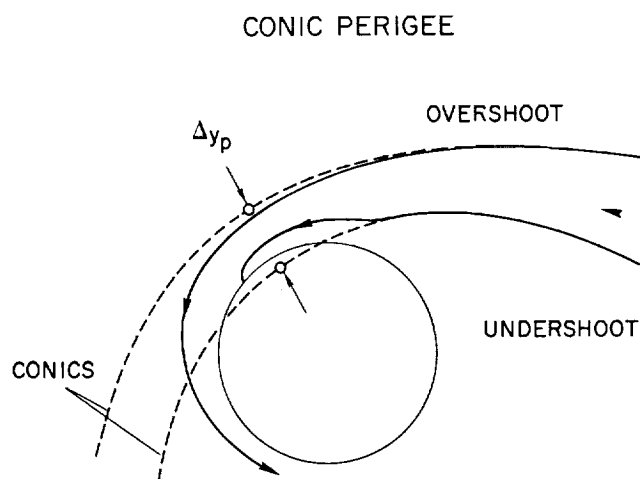
Figure 1

EFFECT OF ENTRY SPEED UPON CORRIDOR DEPTH
NONLIFTING VEHICLE, $G_{MAX}=10$

Figure 2
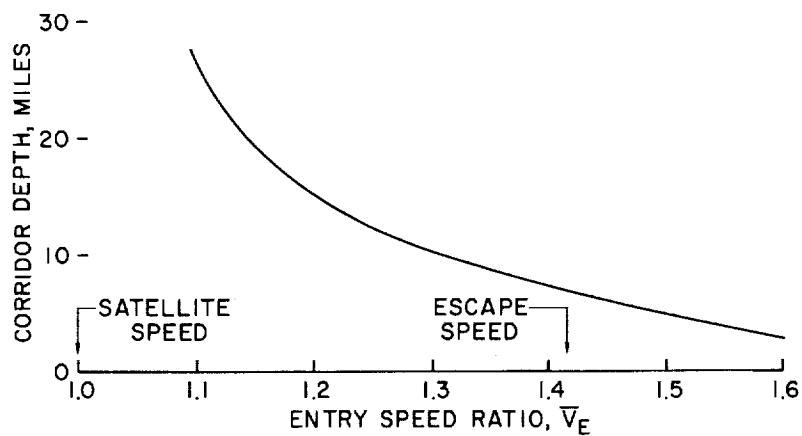
CORRIDOR DEPTH FOR NONLIFTING
VEHICLES
$\overline{V}_E = \sqrt{2}$
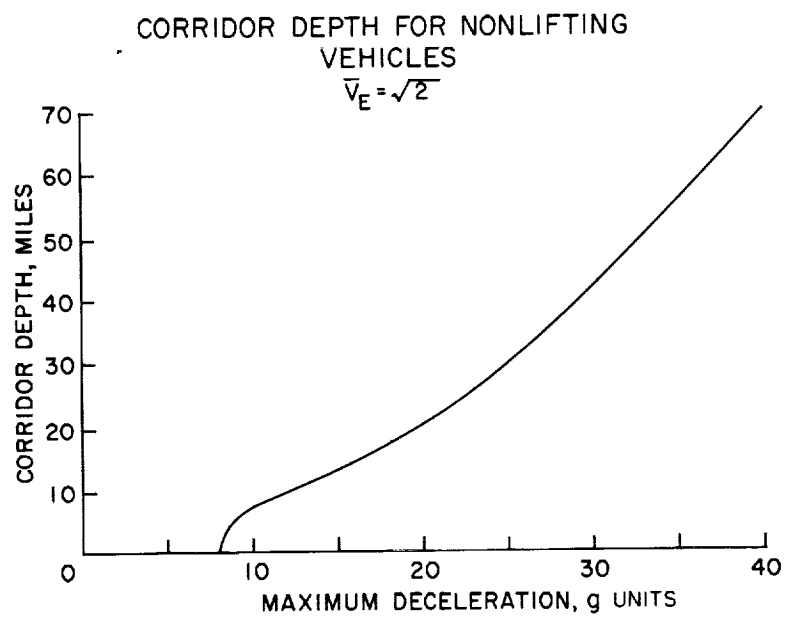
Figure 3

CORRIDOR DEPTHS FOR LIFTING VEHICLES
$\overline{V}_E = \sqrt{2}$; $G_{MAX} = 10$

Figure 4

L
1
0
9
0
C

CONVECTIVE HEATING DOMAINS

Figure 5

STATE OF FLOW
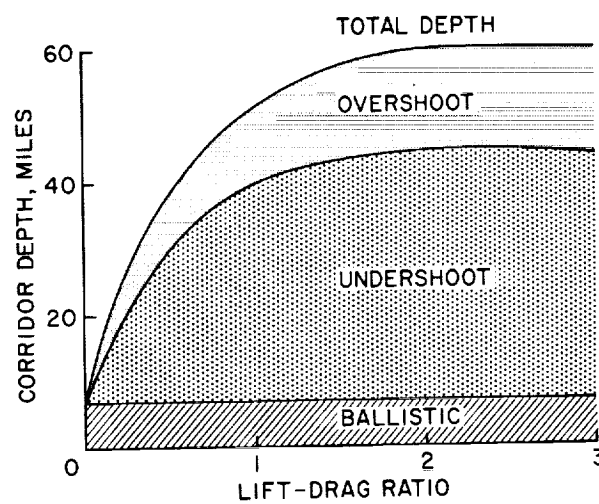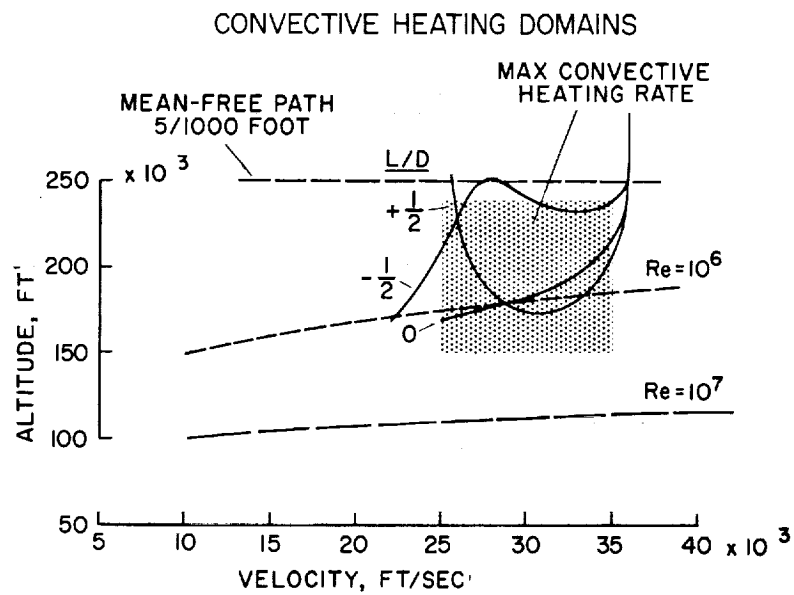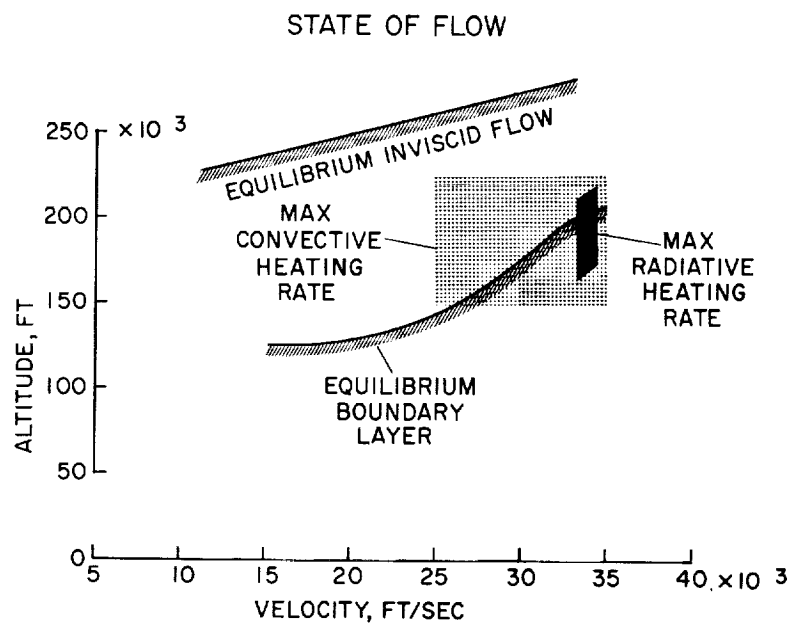
Figure 6

16

HEATING HISTORIES

$$L/D = \pm \frac{1}{2}, \overline{V}_E = \sqrt{2}, \frac{W}{C_D AR} = 56$$
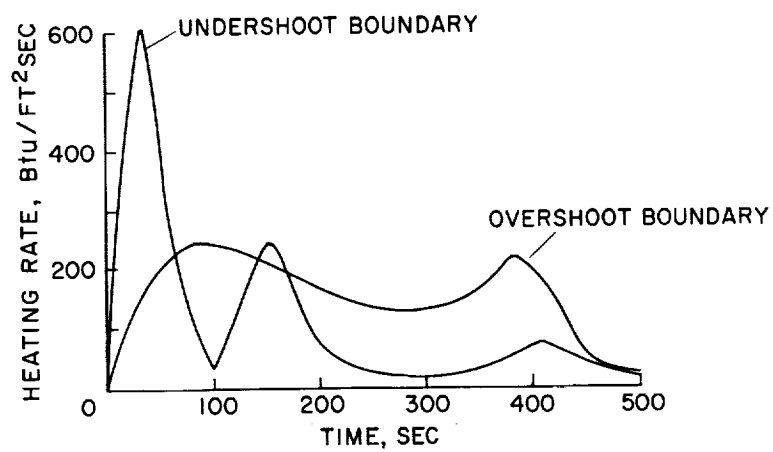
Figure 7

LIFTING BODIES USED IN ANALYSIS

$$C_D = C_{D_0} + \left(C_{D_{MAX}} - C_{D_0}\right) SIN^3 \alpha$$

$$C_L = \left(C_{D_{MAX}} - C_{D_0}\right) SIN^2 \alpha \, COS \alpha$$
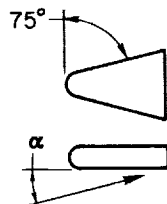
$C_{D_0} = $ NOSE DRAG + LEADING EDGE DRAG

$C_{D_{MAX}} = 1.7$

W = 6000 LB
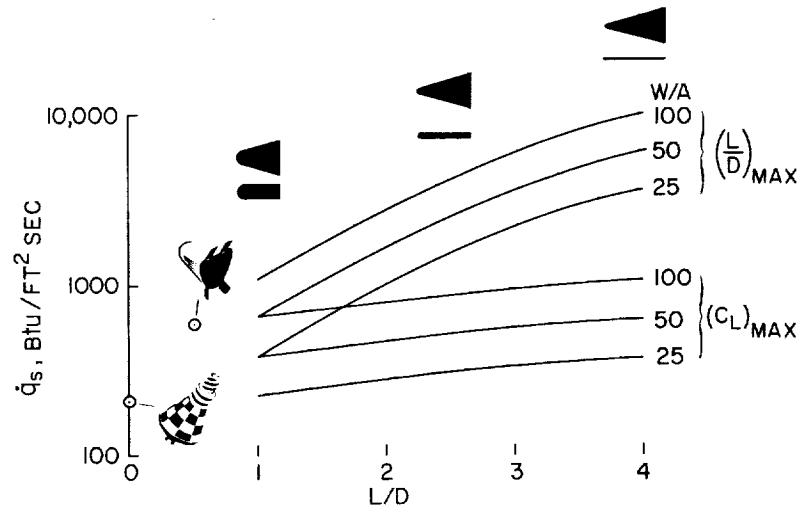
L/D = 1, 2, 3, 4

Figure 8

VEHICLE PARAMETERS
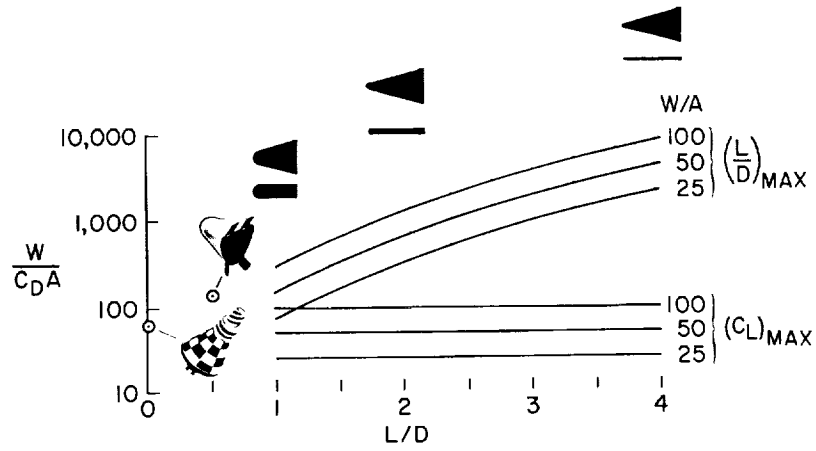
Figure 9

STAGNATION POINT HEATING RATE
UNDERSHOOT BOUNDARY, $G_{MAX} = 10$

Figure 10

HEAT ABSORBED BETWEEN ESCAPE AND
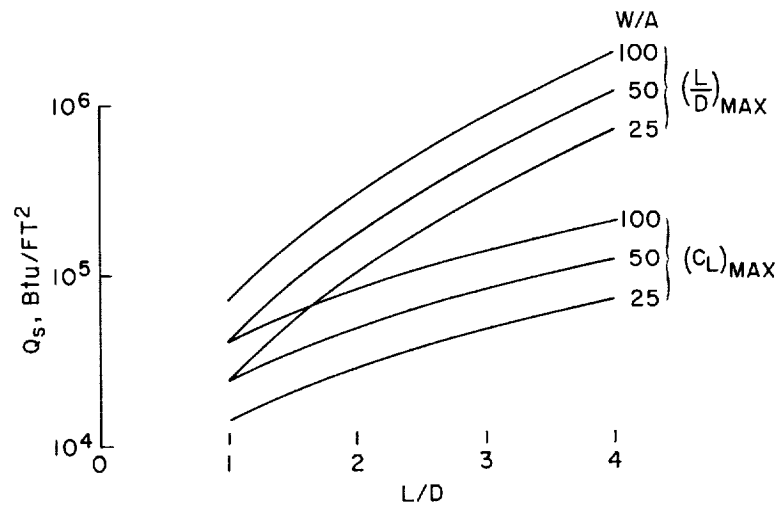SATELLITE SPEED
UNDERSHOOT BOUNDARY, $G_{MAX}=10$

Figure 11

STAGNATION POINT HEATING
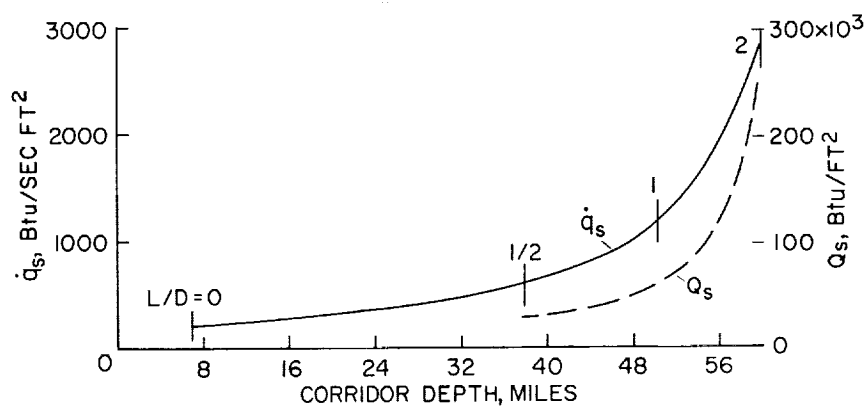UNDERSHOOT BOUNDARY, $G_{MAX}=10$, W/A = 100 LB

Figure 12.